

Towards electron spin resonance of mechanically exfoliated graphene

Luka Ćirić*, Andrzej Sienkiewicz**, Bálint Náfrádi, Marijana Mionić, Arnaud Magrez, and László Forró

Institute of Physics of Complex Matter, EPFL, Lausanne, Switzerland

Received 12 May 2009, revised 3 July 2009, accepted 23 September 2009

Published online 13 November 2009

PACS 68.37.Ps, 75.70.Ak, 76.30.Mi, 76.30.Pk

* Corresponding author: e-mail luka.ciric@epfl.ch, Phone: +41216937936, Fax: +41216934470.

** e-mail andrzej.sienkiewicz@epfl.ch

We have attempted to prepare graphene samples by mechanical exfoliation of HOPG (highly oriented pyrolytic graphite) using scotch tape. Random testing of the flakes by AFM has shown in majority single layer graphene. Nevertheless, the presence of ultrathin graphite cannot be excluded in the large assembly of flakes needed for electron spin resonance (ESR) measurements. Graphene flakes sitting on ESR-silent scotch tapes were stacked parallel to form a multilayer sandwich. The ESR measurements performed in the 4–300 K range yielded narrow Lorentzian line.

The spin susceptibility was decreasing linearly with decreasing temperature as expected for the conical band dispersion of graphene. Below 70 K the spin susceptibility started to deviate from the linear temperature dependence and a Curie-like behavior was observed. This contribution to the susceptibility is due to the existence of defects or impurities, which are in strong exchange coupling limit with conduction electrons. The temperature dependence of the linewidth suggests Elliott's mechanism for spin relaxation in graphene flakes.

© 2009 WILEY-VCH Verlag GmbH & Co. KGaA, Weinheim

1 Introduction The recent discovery of graphene [1], the ultimate two-dimensional hexagonal structure of carbon atoms, has stimulated vast theoretical and experimental activities. The band dispersion has a conical shape; the completely full and empty parts touch each other in a point at the Fermi level, rendering graphene a zero gap semiconductor [2]. Such peculiarities of the band structure are accompanied by the observation of exceptionally high carrier mobility, unconventional quantum Hall effect [3], resilience to very high electrical current densities [4], etc. The very good crystallinity of graphene results in the absence of Anderson localization at low temperatures [5] and a very high Young's modulus [6]. The potential applications are ranging from reinforcements in composite materials [7] through transparent electrodes [8] to field effect transistors [9]. The majority of the experimental studies have focused on transport properties of graphene. In contrast, systematic studies of its magnetic properties are badly missing. Interestingly, some theoretical predictions claim that the defect-mediated magnetism of graphene can give rise either to ferromagnetic or antiferromagnetic ordering, depending on whether the defects correspond to the same or to different sublattices of the bipartite honeycomb lattice [10]. Other

studies predict an alignment of the localized spins along the zigzag edges of graphene [11]. This might result in ferromagnetic order in graphene nano-ribbons with potential applications in spintronics.

Here, we present an electron spin resonance (ESR) study of mechanically exfoliated graphene. ESR is a technique which can be used to detect paramagnetic species. From the ESR signal one can identify different contributions to the overall magnetism of the sample, coming from the conduction electrons and defects.

It is customarily accepted that the highest quality of graphene samples can be obtained via micromechanical cleavage technique [1] of highly oriented pyrolytic graphite (HOPG). However, the yield of this method is too low for fabrication of nanodevices at large scale and for fundamental studies which need a big sample volume, like NMR. Fortunately, ESR has a high sensitivity (10^{10} spins/G) so one can attempt to measure the magnetic response of a limited quantity of graphene. In this work, we report magnetic susceptibility, g -factor and ESR linewidth as a function of temperature of a large assembly of HOPG derived graphene using the scotch-tape technique.

2 Materials and methods For sample preparation we used HOPG and a high purity, ESR-silent 12.5 mm wide Kapton scotch tape. Firstly, a thin piece of HOPG was repeatedly pressed and removed along the scotch tape. Only pieces with optically “non-visible” graphitic particles were collected. To prove the presence of ultrathin graphite and graphene monolayers, occasionally the sample from the scotch tape was transferred to Si/SiO₂ wafer and further characterized with AFM. A typical AFM topography is shown in Fig. 1. From these measurements the height of the layer is estimated to be $\sim 1.2 \pm 0.2$ nm which is in agreement with data from literature for a monolayer of graphene [1]. Although the representative AFM scans show good sample quality, we cannot rule out that the large assembly contains not only monolayers of graphene but also ultra-thin graphite flakes. For simplicity, hereafter we use the term graphene for our sample, keeping in mind the possible contamination with ultrathin graphite.

A large number of such scotch-tape pieces were “sandwiched” for ESR measurements. The obtained macroscopic sample was placed in a 2.9 mm ID and 4 mm OD quartz tube (see sketch in Fig. 2), which was sealed under vacuum. Low temperature ESR measurements were performed using a standard X-band ESR spectrometer equipped with a helium gas-flow cryostat for low temperature measurements.

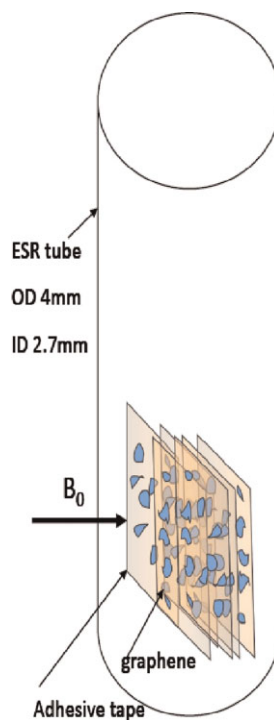


Figure 2 (online color at: www.pss-b.com) Sketch of the sample configuration for ESR measurement: layers of graphene flakes on scotch tapes are placed in the 4 mm OD \times 2.9 mm ID ESR capillary.

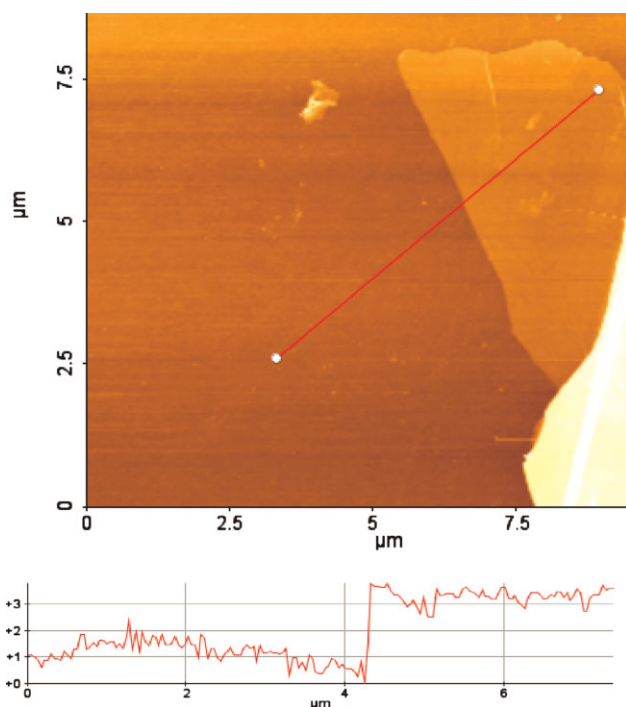


Figure 1 (online color at: www.pss-b.com) AFM topography acquired for a graphene flake deposited on SiO₂ substrate after its removal from the Kapton tape. The brighter region in the upper right side is the graphene layer. The height profile (lower image) was done along the line marked on the image.

3 ESR results and discussion The ESR measurements were performed in the temperature range of 4–300 K. Except for very low temperatures (4–20 K), we have found a single Lorentzian line. (In the case of bulk graphite the ESR line is Dysonian due to the skin effect.) A typical spectrum measured at $T=150$ K is shown in Fig. 3. The spin susceptibility, proportional to the double integrated ESR line, reveals a temperature dependence close to the expected one for graphene (Fig. 4), that is $\chi \sim T$. However, as seen in Fig. 4, at temperatures below 70 K, χ increases revealing a Curie-like behavior. Since we observe a single ESR line (above 20 K) we interpret this as the strong coupling limit between paramagnetic defects and conduction electrons in graphene. It is difficult to give an absolute value for the spin susceptibility, since we cannot measure the mass of the sample. If we suppose that at 300 K χ is in the range of 1×10^{-8} emu/g measured for graphite or multi walled carbon nanotubes (MWCNTs), then the Curie tail corresponds to 4×10^{16} spins/cm³. This defect concentration is two orders of magnitude lower than that measured for MWCNTs [12]. This confirms a relatively low concentration of defects and localized states of pristine graphene compared to other carbon nanostructures. After the subtraction of the Curie contribution a T -linear susceptibility is observed in the entire temperature range (blue squares in Fig. 4).

This behavior correlates with the graphene’s conical band dispersion having the Fermi level in the vicinity of the

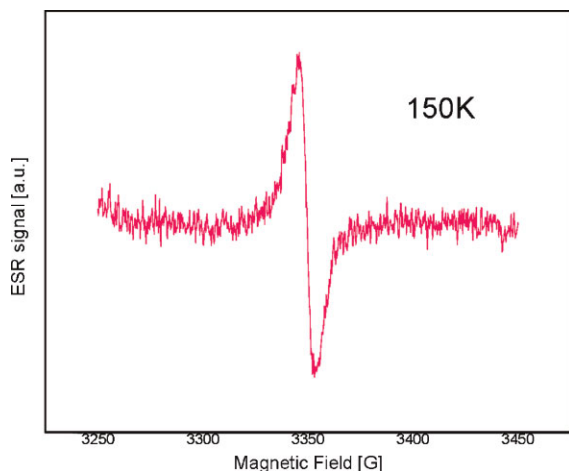


Figure 3 (online color at: www.pss-b.com) Typical ESR line recorded at 150 K for the assembly of stacked graphene flakes. The ESR line has a Lorentzian shape; it is centered on $g \sim 2$, having a linewidth of 6.5 G.

neutrality point. Assuming that Zeeman energy is much smaller than $k_B T$ and that temperature is low enough that we are in the linear dispersion regime, it is simple to show that the susceptibility follows linear variation with temperature:

$$\chi \approx (\mu_B^2 g / \pi \alpha) k_B T$$

where α represents the slope of the band dispersion in k -space.

We have to notice, that the finite intercept at $T=0$ of our data is in disagreement with the above description. This discrepancy may come from the “contamination” of graphene with ultrathin graphitic flakes, or from an unintentional doping of graphene. At this point we cannot pinpoint the origin of this “non-graphene-like” contribution to χ .

The very weak T -dependence of ΔH in the T -range where defects do not interfere with the conduction electrons (see Fig. 5), corroborates well with the weak T -dependence of the electrical resistivity [13]. Namely, Tan et al. have reported a 10% increase of resistivity between 300 K and 30 mK at the neutrality point, and 35% decrease in the n -doped regime. We cannot determine the Fermi level for our sample, nevertheless the fact that χ follows a linear T -dependence suggests that we are close to the neutrality point. We can safely presume that the resistivity of our sample has also a weak T -dependence. This observation would suggest that the spin relaxation in graphene is governed by the Elliott mechanism like in conventional metals [14]. From the CESR linewidth we can determine the characteristic spin-lattice relaxation time of the system. Assuming $1/T_1 = 1/T_2 = \gamma_e \Delta H$, where $\gamma_e = 28.0$ GHz/T is the electron gyromagnetic ratio, $1/T_1$ electron spin-lattice relaxation rate, and $1/T_2$ is the spin-spin or transversal relaxation rate, we find that T_1 relaxation time is of the order of 55 ns deduced from 6.5 G of ΔH at 150 K. This value clearly differs from the spin lifetime

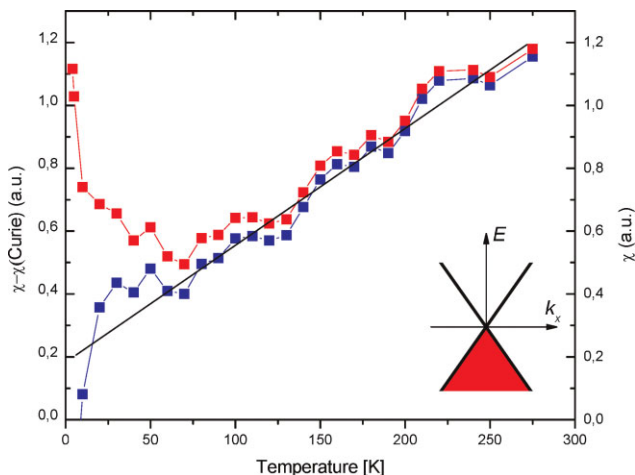


Figure 4 (online color at: www.pss-b.com) Temperature dependence of the spin susceptibility of graphene: the overall spin susceptibility (red squares) and the spin susceptibility after the subtraction of the Curie contribution (blue squares). The inset shows the sketch of the conical band-structure model in the vicinity of the neutrality point in graphene.

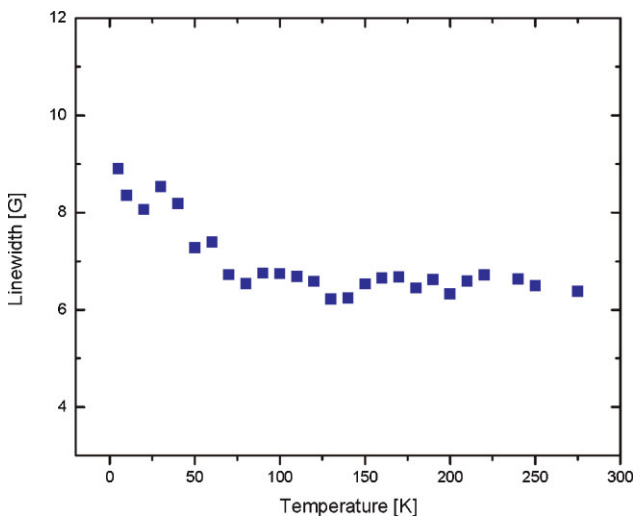


Figure 5 (online color at: www.pss-b.com) Temperature evolution of the ESR linewidth of graphene. The temperature independent contribution is coming from the conduction electrons while the slight broadening starting around 70 K is due to the dipolar broadening coming from localized spins.

of 100 ps obtained by Tombros et al. [15] in a field effect transistor geometry. It is difficult to find the source of this discrepancy, but it is possible that in their case the substrate has a strong effect on the spin-flip process.

The strong coupling of the defects to the conduction electrons at low temperatures affects the ESR linewidth as well. In the temperature range 4–70 K, the ESR linewidth diminishes from 9 to ~ 6.5 G (Fig. 5) on heating which could be interpreted as motional narrowing of the dipolar linewidth of localized spins.

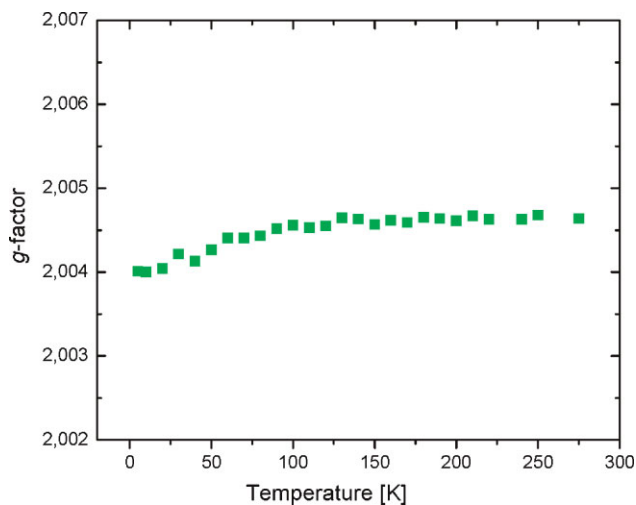


Figure 6 (online color at: www.pss-b.com) Temperature dependence of the g -factor of graphene.

The temperature dependence of the g -factor (see Fig. 6) also reveals two distinct temperature ranges. At temperatures below ~ 70 K, the g -factor diminishes with decreasing temperature, whereas at temperatures higher than 70 K, the g -factor remains independent of temperature. In the framework of the proposed strong coupling limit we can estimate $g_{\text{imp}} \sim 2.0034$ at $T = 4$ K.

4 Conclusions We have reported ESR measurements on a large assembly of mechanically exfoliated graphene flakes using scotch-tape. The spin susceptibility shows the characteristics expected from band structure calculations, that is $\chi \sim T$. The finite intercept of χ might indicate a non-negligible presence of ultrathin graphitic flakes in our sample, although the overall characteristics (χ , ΔH and g -factor) are markedly different from the properties of graphite [16].

Acknowledgements This work was performed within the framework of the European network “IMPRESS”. Fruitful discussions with V. Stevanovic are gratefully acknowledged.

References

- [1] K. S. Novoselov, A. K. Geim, S. V. Morozov, D. Jiang, Y. Zhang, S. V. Dubonos, I. V. Grigorieva, and A. A. Firsov, *Science* **306**, 666 (2004).
- [2] P. R. Wallace, *Phys. Rev.* **71**, 622 (1947).
- [3] K. S. Novoselov, A. K. Geim, S. V. Morozov, D. Jiang, M. I. Katsnelson, I. V. Grigorieva, S. V. Dubonos, and A. A. Firsov, *Nature* **438**, 197 (2005).
- [4] A. K. Geim and K. S. Novoselov, *Nature Mater.* **6**, 183 (2007).
- [5] K. S. Novoselov, S. V. Morozov, T. M. G. Mohinddin, L. A. Ponomarenko, D. C. Elias, R. Yang, I. I. Barbolina, P. Blake, T. J. Booth, D. Jiang, J. Giesbers, E. W. Hill, and A. K. Geim, *Phys. Status Solidi B* **244**, 4106–4111 (2007).
- [6] C. Lee, X. Wei, J. W. Kysar, and J. Hone, *Science* **321**, 385–388 (2008).
- [7] S. Stankovich, D. A. Dikin, G. H. B. Dommett, K. M. Kohlhaas, E. J. Zimney, E. A. Stach, R. D. Piner, S. B. T. Nguyen, and R. S. Ruoff, *Nature* **442**, 282–286 (2006).
- [8] X. Wang, L. J. Zhi, and K. Mullen, *Nano Lett.* **8**, 323 (2008).
- [9] T. J. Echtermeyer, M. C. Lemme, J. Bolten, M. Baus, M. Ramsteiner, and H. Kurz, *Eur. Phys. J. Special Topics* **148**, 19–26 (2007).
- [10] O. V. Yazyev and L. Helm, *Phys. Rev. B* **75**(12), 125408 (2007).
- [11] O. V. Yazyev and M. I. Katsnelson, *Phys. Rev. Lett.* **100**, 047209 (2008).
- [12] O. Chauvet, L. Forro, W. Bacsá, D. Ugarte, B. Doudin, and W. A. de Heer, *Phys. Rev. B* **52**, R6963 (1995).
- [13] Y. W. Tan, Y. Zhang, H. L. Stormer, and P. Kim, *Eur. Phys. J. Special Topics* **148**, 15–18 (2007).
- [14] F. Beneu and P. Monod, *Phys. Rev. B* **19**, 911–916 (1979).
- [15] N. Tombros, C. Jozsa, M. Popinciuc, H. T. Jonkman, and B. J. van Wees, *Nature* **448**, 571–574 (2007).
- [16] D. L. Huber, R. R. Urbano, M. S. Sercheli, and C. Rettori, *Phys. Rev. B* **70**, 125417 (2004).